Atmospheric aerosol deposition fluxes over the Atlantic Ocean: A GEOTRACES case study

Jan-Lukas Menzel Barraqueta[1], Jessica K. Klar[2,3], Martha Gledhill[1], Christian Schlosser[1], Rachel Shelley[4,5,6], Hélène Planquette[5], Bernhard Wenzel[1], Geraldine Sarthou[5], Eric P. Achterberg[1]

5 [1] *GEOMAR, Helmholtz Centre for Ocean Research Kiel, Germany*

[2] *Ocean and Earth Science, National Oceanography Centre, University of Southampton, European Way, Southampton SO14 3ZH, UK*

[3] *LEGOS, Université de Toulouse, CNES, CNRS, IRD, UPS, 14 Avenue Edouard Belin, 31400 Toulouse, France*

[4] *Department of Earth, Ocean and Atmospheric Science, Florida State University, 117 N Woodward Ave,Tallahassee,*
10 *Florida, 32301, USA*

[5] *Laboratoire des Sciences de l'Environnement Marin, UMR 6539 LEMAR (CNRS/UBO/IRD/IFREMER),Institut Universitaire Européen de la Mer, Technopôle Brest-Iroise, Plouzané 29280,LEMAR, UMR 6539, Plouzané, France*

[6] *School of Geography, Earth and Environmental Sciences, University of Plymouth, Drake Circus, Plymouth, PL4 8AA, UK*

Correspondence to: Jan-Lukas Menzel Barraqueta (jmenzel@geomar.de)

15 **Abstract.**

Atmospheric deposition is an important source of micronutrients to the ocean, but atmospheric deposition fluxes remain poorly constrained in most ocean regions due to the limited number of field observations of wet and dry atmospheric inputs. Here we present the distribution of dissolved aluminium (dAl), as a tracer of atmospheric inputs, in surface waters of the Atlantic Ocean along GEOTRACES sections GA01, GA06, GA08, and GA10. We used the surface mixed layer
20 concentrations of dAl to calculate atmospheric deposition fluxes using a simple steady state model. We have optimized the Al fractional aerosol solubility, dAl residence time within the surface mixed layer and depth of the surface mixed layer for each separate cruise to calculate the atmospheric deposition fluxes. We calculated the lowest deposition fluxes of 0.15 ± 0.1 and 0.27 ± 0.13 g m^{-2} yr^{-1} for the South and North Atlantic Ocean (> 40°S and > 40°N), respectively, and highest fluxes of 2.67 ± 1.96 and 3.82 ± 2.72 g m^{-2} yr^{-1} for the South East Atlantic and tropical Atlantic Ocean, respectively. Overall, our
25 estimations are comparable to atmospheric dust deposition model estimates and reported field-based atmospheric deposition estimates. We note that our estimates diverge from atmospheric dust deposition model flux estimates in regions influenced by riverine Al inputs and in upwelling regions. As dAl is a key trace element in the GEOTRACES Programme, the approach presented in this study allows calculations of atmospheric deposition fluxes at high spatial resolution for remote ocean regions.

30 .

1 Introduction

Atmospheric deposition is a major source of micronutrients, especially iron, to the surface ocean (Martin et al., 1991; Moore et al., 2004). Aerosol deposition of iron in the tropical and subtropical North Atlantic stimulates N_2 fixation (Moore et al.,

5   2009), and in high latitude waters with high nitrate low chlorophyll conditions it can enhance primary productivity (Baker et al., 2013). Consequently, atmospheric deposition is considered to support up to 50 % of global export production (Jickells et al., 2014). Therefore, by supplying growth-limiting elements to marine micro-organisms, atmospheric deposition can have important direct impacts on the marine carbon cycle and indirectly influence global climate (Mahowald et al., 2014).

The size distribution of mineral dust is considered a continuum. However, mineral dust is often described to have a bimodal

10 size distribution and thus aerosols are classified into a fine (radius 0.1- 0.25 μM) or coarse mode (radius 1 – 2.5 μM) (Maring et al., 2003). The classification facilitates us to assign aerosol deposition velocities for the aerosol size classes for the quantification of dry deposition fluxes (Slinn and Slinn, 1980). Mineral dust mobilization mainly depends on vegetation cover, surface soil moisture content, and wind friction speed (Mahowald et al., 2014; Zender et al., 2003). Once mobilized by wind and lofted into the troposphere, mineral dust can be transported thousands of kilometres from source regions

15 following major air mass movements. In the North Atlantic the trade winds transport dust from North Africa to the Caribbean and Americas (Prospero et al., 2010) in about one week (Ott et al., 1991). Along the transport path of atmospheric aerosols, the size distribution of aerosol tends to decrease with increasing distance from the source regions. Chemical and physical transformation processing of aerosol in clouds, such as photo-reduction and dissolution, can enhance the fraction of trace metals that are released upon deposition into the surface ocean (Duce and Tindale, 1991). Thus, the degree of

20 atmospheric processing can be a critical factor in determining the impact of atmospheric deposition on marine ecosystems (Baker and Croot, 2010; Mahowald et al., 2011).

In the Atlantic Ocean, mineral dust deposition is highest in tropical regions located downwind of the major aerosol source regions of the Sahara Desert and Sahel (Jickells et al., 2005; Prospero and Carlson, 1972). Moreover, the Intertropical Convergence Zone (ITCZ) in the Atlantic Ocean (located at ~ 5 – 10 °N in winter and summer, respectively) features intense

25 wet deposition which effectively strip the aerosols from the atmosphere, thereby depositing trace elements to the surface ocean in solution (Kim and Church, 2002; Schlosser et al., 2014). Other important mineral dust source regions include the Namib Desert and Patagonia for the South Atlantic Ocean (Chance et al., 2015; Mahowald et al., 2005; Wagener et al., 2008). In remote marine areas such as the far North and South Atlantic, removed from major desert dust sources, aerosols are of a mixture of marine origin, shipping emissions, industrial and agricultural emissions from the continents (Baker et al.,

30 2013; Chance et al., 2015; Shelley et al., 2017a), seasonal emissions of proglacial till (Bullard et al., 2016) and occasional volcanic ash emissions (Achterberg et al., 2013). In addition, aerosols in these remote regions may also have a mineral dust component, depending on the meteorological conditions (Prospero, 1996a).

Atmospheric deposition flux determination have a relatively high uncertainty (Zender et al., 2003) due to large inter-annual and inter-seasonal variabilities. Several approaches are used to calculate atmospheric deposition fluxes from geochemical tracers or proxies (Anderson et al., 2016). Geochemical methods determine atmospheric deposition fluxes from elemental concentrations in aerosols and/or rain, or chemical concentrations or signatures of tracers of atmospheric deposition in

5   seawater (Anderson et al., 2016). A commonly used geochemical method to determine total (wet + dry) deposition fluxes is to measure elemental concentrations in aerosols collected on filters and in rain water, and multiplying the aerosol concentration data with deposition velocities (dry deposition flux) and the rainwater concentration data by a precipitation rate (wet deposition flux) (Baker et al., 2003; Prospero, 1996a; Shelley et al., 2017b). Atmospheric dry deposition fluxes are subject to a 2-3 fold uncertainty due to the use of a single deposition velocity in the flux calculation (Duce et al., 1991) thus

10   not taking into account the varying deposition velocity of different mineral dust sizes. However, when size segregated sampling approaches are used more than one deposition velocity is applied, thereby decreasing the uncertainty in the calculated deposition flux. The uncertainty may be even larger for wet deposition fluxes because of the uncertainties associated with precipitation rates and scavenging ratios (Shelley et al., 2017a). A different approach that tries to reduce the uncertainties associated with the deposition velocity and precipitation rates uses the inventory of ^{7}Be in the surface mixed

15   layer and the ratio of trace elements to ^{7}Be in aerosols to calculate atmospheric deposition fluxes on seasonal timescales (Kadko et al., 2015; Kadko and Prospero, 2011). Other approaches used to determine atmospheric fluxes of trace elements use particles collection by sediment traps (Jickells et al., 1998; Kohfeld and Harrison, 2001) or analyse mineral dust tracers in surface ocean waters (Dammshäuser et al., 2011). Modern atmospheric models take into account aerosol characteristics (e.g. size distribution, particle type) and field observations to estimate atmospheric deposition fluxes (Mahowald et al., 2005;

20   Zender et al., 2003; Zhang et al., 2015). Often, modelling approaches simulate atmospheric deposition fluxes more accurately in regions downwind from the main aerosol sources (Huneeus et al., 2011; Wagener et al., 2008) because the aerosol characteristics, due to extensive datasets in these regions, are better constrained in proximity to their source. Modelled atmospheric deposition fluxes rely on satellite-derived climatologies which suffer from interferences from cloud coverage.

25   In this manuscript we present surface ocean dAl concentration data for the Atlantic Ocean and use these to calculate atmospheric deposition fluxes using the MADCOW model (Measures and Brown, 1996). The strength of this approach is that it can be used to fill gaps where there are relatively few direct aerosol observations and that with just one parameter it allows the calculation of total atmospheric deposition fluxes (wet + dry). This study compares the MADCOW model outputs with field and model-derived atmospheric deposition flux estimates from the North to the South Atlantic Ocean. We provide

30   some of the first atmospheric deposition fluxes based on high-resolution surface mixed layer concentrations of dAl for remote regions including the Labrador Sea, South East Atlantic and South Atlantic Ocean (ca. 40°S). Our results are discussed in light of the assumptions and limitations of the MADCOW model, and compared to available atmospheric deposition flux estimates from modelling and geochemical approaches.

2. Methods

2.1 Regional, sampling, and processing settings

Seawater samples for dAl were collected during the GEOTRACES section cruises GA01, GA06, GA08, and GA10 (Figure 1). GEOTRACES section GA01 sailed aboard the research vessel Pourquoi Pas? on 15 May (2014) from Lisbon (Portugal)

5 and arrived on 30 June (2014) in St. John´s (Canada). GEOTRACES section GA06 sailed aboard RRS Discovery on 7 February (2011) from Tenerife (Canary Islands, Spain) and returned on 19 March (2011) to Tenerife. GEOTRACES section GA08, on board FS Meteor, sailed from Walvis Bay (Namibia) on 14 November (2015) and returned there on 27 December (2015). GEOTRACES section GA10, on board RRS James Cook, sailed on 24 December (2011) from Port Elizabeth (South Africa) and arrived on 27 January (2012) in Montevideo (Uruguay). The four expeditions crossed several biogeochemical

10 provinces (Longhurst, 2010) which are shown in Figure 1 and listed in Table S1 along with their geographical boundaries, ecological and physical properties.

In total, seawater samples were collected at 108 stations, with 32 stations sampled during GA01, 14 stations during GA06, 52 stations during GA08 and 18 stations during GA10. Although the different teams used slightly different CTD set ups for sampling the seawater (Table S2), all samples were collected using trace metal clean CTD rosettes and following the

15 GEOTRACES sampling protocols (Cutter et al., 2017). All seawater samples for the determination of dAl were collected in 125 mL low density polyethylene bottles (LDPE; Nalgene) cleaned using a three-step wash protocol (Cutter et al., 2017). After collection, the samples were acidified to pH 1.8 with ultra clean hydrochloric acid (UpA, Romil) and double bagged until analysis. Analysis of dAl during GA01, GA06, and GA10 used the flow injection analysis (FIA) method developed by Resing and Measures (1994) and further modified by Brown and Bruland (2008). Dissolved Al during GA08 cruise was analysed using the batch

20 lumogallium method (Hydes and Liss, 1976). The analytical figures of merit for the dAl datasets can be found in Table S2.

2.2 Atmospheric deposition flux determinations: The MADCOW model

The MADCOW (Measurement of Aluminium for Dust Calculation in Ocean Waters) model (Measures and Vink, 2000;

25 Measures and Brown, 1996) determines atmospheric deposition fluxes to the surface ocean from the concentration of dAl in the surface mixed layer. The primary model assumption is that dAl in the surface waters is in steady state with respect to inputs from soluble Al provided by the dissolution of mineral dust on contact with seawater and rain deposition, and removal via scavenging of Al onto particle surfaces, and subsequent transfer to depth by sinking. The model itself is provided by the following equation (Eq.1):

30   Eq.1 $G = \frac{[Al] \times MLD}{\tau \times S \times D}$ (1)

Where G is the total dust flux in g m^{-2} yr^{-1}, [Al] is the concentration of dAl (nM) in the surface mixed layer, MLD is the depth of the mixed layer in meters (m), τ is the residence time in years (yr), S is the fractional solubility of Al in dust (%),

and D is the concentration of Al in dust (mol g^{-1}). We describe how each parameter is derived for each of the cruises in the following sections and describe the assumptions used by the MADCOW model for the determination of the atmospheric deposition fluxes.

2.2.1 Quantification of surface mixed layer depths

We used two different MLDs. First, a measured mixed layer depth (MLDms) was obtained for each station using a potential density difference criterion $\Delta\sigma\ \theta = 0.125$ kg m^{-3} (Monterey and Levitus, 1997) calculated from the salinity and temperature retrieved from the sensors mounted in the CTDs. Second, annual (MLDar) and seasonal (MLDwi, MLDsp, MLDsu and MLDau, for winter, spring, summer, and autumn, respectively) MLDs were extracted for each station of the four cruises in a 1 x 1 degree bin in latitude and longitude from the Argo mixed layer climatology (http://mixedlayer.ucsd.edu/) (Holte et al., 2017).

2.2.2 Fractional solubility of Al

Seasonal (April to June and September to November) Al fractional solubilities were obtained from the compilation of Baker et al. (2013), based on aerosol samples collected at high spatial resolution over several years in the Atlantic Ocean. The soluble fraction was based on the results of an ammonium acetate leach at pH 4.7 for 1-2 h, following Sarthou et al. (2003). Baker et al. (2013) divided the Atlantic Ocean into various regions and sub-regions (Figure S2) based on air mass back trajectories and the relative contribution of the air masses over the two seasons in each region. Along with Figure S2 we provide an explanatory note on the relative contribution of each air mass for each region which we then compiled in Table S3. They calculated the fractional Al solubility for each sub region. Baker et al. (2013) provide a good spatial coverage of the Atlantic Ocean, thus allowing us to assign values of Al fractional solubility for different biogeochemical regions (Figure 1) based on field observations. However, the aerosols Al fractional solubility might not be representative over an annual timescale due to, for example, the pulses of Saharan dust and where the mineral dust falls which is related to the position of the ITCZ. Yet, it is still the largest dataset on aerosol Al fractional solubility over the Atlantic Ocean. We produced a single weighted averaged aerosol Al fractional solubility percentage value for each area of interest based on the Al fractional solubility for each air mass to the relative contribution of that air mass to a certain area (Table S3). Furthermore, we assumed that the chosen Al solubility was representative for the whole annual cycle as our atmospheric aerosol deposition flux estimates are given in g m^{-2} y^{-1}. As the compilation of Baker et al. (2013) does not cover regions north of 50°N in the North Atlantic, we used Al fractional solubilities from Shelley et al. (2017a) derived from aerosol samples collected during the GA01 cruise.

2.2.3 Al residence time in the surface mixed layer

The residence time is defined as the ratio of the dAl inventory in the surface mixed layer to the rate of input or removal. Residence times of dAl in the surface mixed layer were obtained from Han et al. (2008) and were derived using model simulations using the Biogeochemical Elemental Cycling (BEC) ocean model (Moore et al., 2004). The dAl residence times

5   provided by Han et al. (2008) take into account Al sources to the surface mixed layer from atmospheric deposition, advection, and mixing. We have chosen the residence times from Han et al. (2008) as they are based on an extensive surface water dAl observational database, including a total of 41 research expeditions (22 in the Atlantic Ocean) up to the year 2002. The MADCOW model used in our study does not account for advection and mixing processes which, for example, occurs in equatorial regions as waters of higher dAl concentrations are advected into low dAl concentration waters (van Hulten et al.,

10   2013). Thus, the use of modelled residence times which account for advection and mixing sources could partially counterbalance the error associated with our modelled atmospheric deposition fluxes.

3. Results and Discussion

3.1 Mixed layer depth (MLD)

15   The surface mixed layer is considered a quasi-homogenous layer based on physical properties (S and T). The properties display gradients at the bottom of the layer. The bottom depth of the surface mixed layer varies due to atmospheric forcing, with turbulent mixing caused by wind stress (Risien and Chelton, 2008), convection caused by heat exchange (Yu and Weller, 2007), in addition to salinity changes due to evaporation and precipitation at the surface (Schanze et al., 2010). Thus, the thickness of the MLD is an indication of the amount of water that directly interacts with the atmosphere.

20   Figure 2 shows a box whisker plot with the quantified MLDs for each of the four study regions. Table S4 shows the calculated MLDs for each station and Figure S3 (a,b,c,d) shows a comparison plot for each cruise between MLDms, MLDar, MLDmw (mixed layer depth original MADCOW model) and the Argo average MLD during the season when each cruise took place.

In the North Atlantic (GA01) and South Atlantic (GA10) Ocean, large differences were observed between median MLDms

25   and MLDar with a difference of 77 and 20 m, respectively. Smaller differences were detected between median MLDms and MLDar in the tropical (GA06) and Southeast Atlantic (GA08) Ocean with a difference of 7 and 10 m, respectively. Maximum MLDar and MLDms were greatest in the North Atlantic (up to 218 m), followed by the South Atlantic (106 m) and the South East Atlantic (83 m) and tropical Atlantic (66 m). The large difference, both in maximum MLDar and in the difference between the median MLDms and MLDar, between the North Atlantic Ocean and the other three study areas was

30   due to strong deep mixing taking place in the North Atlantic Ocean during winter (Kara et al., 2003). In the tropical Atlantic Ocean, the MLD is largely controlled by changes in temperature (net heat flux) and salinity (evaporation to precipitation

ratios) (Chahine, 1992; Webster, 1994). In our study, deeper MLDs relative to shallower MLDs imply that higher quantities of atmospheric aerosols need to be supplied to a specific region in order to maintain the observed dAl concentrations in the MLD.

3.2 Distributions of dAl in the surface mixed layer

5   Figure 3 shows the average dAl concentration in the surface mixed layer along the four sections. Occasionally, when no sample was collected, the closest underway surface water sample collected with a towfish was used. A detailed description for the surface mixed layer dAl concentrations of the four cruises relative to physical and biological parameters is given in the following sections. Overall, a large range in surface dAl concentrations was observed, ranging between < 0.5 nM and 784 nM (median 5.1 nM; n=108 stations). The highest dAl concentrations were observed in the tropical Atlantic Ocean

10   between 1-15° N and ca. 26° W, and in coastal waters off Portugal, Greenland, Argentina, Angola, Democratic Republic of Congo, and Gabon in association with the highest atmospheric inputs and continental inputs (rivers, glacial flour, and ice melt). In contrast, low dAl concentrations (< 5 nM) due to low atmospheric deposition and/or scavenging of dAl by particles were found in the North Atlantic (GA01), in the South East Atlantic (GA08), and in the South Atlantic Ocean (GA10).

3.2.1 Dissolved Al in the surface mixed layer of the North Atlantic Ocean (GA01)

15   Along GEOTRACES GA01 section in the North Atlantic (Figure 1), highest (> 15 nM) dAl surface mixed layer concentrations were found in the North Atlantic Subtropical Gyre region (NAST) off Portugal (stations 1, 2 and 4) and are attributed to riverine inputs from the Tagus estuary (Menzel Barraqueta et al., 2018). An additional source of dAl off Portugal involves episodic deposition of mineral dust originating from the Sahara and Sahel regions (Prospero, 1996a), and wet deposition events as observed during the GA01 cruise (Shelley et al., 2017a). Enhanced dAl surface mixed layer

20   concentrations (> 5 nM) were also observed in the Atlantic Arctic region (ARCT) off Southeast and Southwest Greenland (stations 53 and 61) as a consequence of runoff and ice melt, respectively (Menzel Barraqueta et al., 2018). In addition, enhanced dust inputs delivered from proglacial tills in Greenland occur from June to September (Bullard et al., 2016), coinciding with the time of sample collection off Greenland. Excluding the stations with continental Al inputs, mixed layer dAl concentrations were low, reflecting low contributions of atmospheric deposition (median dAl = 2.9 nM), and were not

25   significantly different from east to west due to differences in the intensity of biological removal processes as described by Menzel Barraqueta et al. (2018). A more detailed explanation on the surface distribution for dAl along the GA01 cruise is given in Menzel Barraqueta et al. (2018). Similarly low concentrations of dAl were observed during the CLIVAR A16N line along 22° W longitude in the eastern North Atlantic in 2003 (Measures et al., 2008), and when re-occupied in 2013 (Barrett et al., 2015), and in the Irminger Basin during GEOTRACES GA02 (Middag et al., 2015).

3.3.2 Dissolved Al in the surface mixed layer of the tropical Atlantic Ocean (GA06)

The tropical Atlantic has a large coverage of dAl measurements, compiled in Han et al. (2008), related to the importance of dust delivering micronutrients (e.g. Fe) to the surface ocean. Along the GEOTRACES GA06 section, dAl concentrations were high and ranged from 8 nM in the North Atlantic Tropical Gyre region (NATR) to 67 nM in the Western Tropical

5   Atlantic region (WTRA). In the southern part of the section at ~8°S, at the boundary between the South Atlantic Gyre (SAG) and the South Equatorial Current (SEC) in the WTRA (Figure 1), dAl displayed low concentrations (~8.8 nM) with elevated salinity (36.54) (Figure 4). The latter region is known to have low rainfall, high rates of evaporation (Yoo and Carton, 1990) and receives large volumes of mineral dust deposition (Prospero, 1996b). Vink and Measures (2001) observed similarly low levels of dAl (8 nM) but somewhat further south at 15°S. Similarly, on the westward transect at ca. 12.5°N, low dAl

10   concentrations were observed (down to 8 nM), associated with enhanced removal of dAl by biogenic particles. Enhanced primary production as a consequence of upwelling of nutrient-rich deep water resulted in a high abundance of biogenic particles; Measures et al. (2015) reported similar conditions for the region. High dAl concentrations (15-28 nM) were found north of 3°S and were related to enhanced deposition of mineral dust as the sampling stations were located along the flow path of the trade winds that carry mineral dust from the Sahara and Sahel regions (Mahowald et al., 2005; Prospero et al.,

15   2002). Maximum concentrations of dAl (up to 68 nM) were observed at ca. 3°N, 26° W (station 14) and coincided with reduced salinity (down to 35) (Figure 4), suggesting freshwater inputs from rainfall occurring in the ITCZ. The ITCZ was positioned between ca. 3°S and 3°N with the core situated at 1°N during the cruise period (Schlosser et al., 2014). Precipitation in the ITCZ effectively scavenges dust from the atmosphere and supplies Al to surface waters in wet deposition (Schlosser et al., 2014). Similarly high dAl concentrations (e.g. up to 74 nM)(Van Der Loeff et al., 1997) for the region have

20   been reported (Barrett et al., 2015; Bowie et al., 2002; Dammshäuser et al., 2011; Measures et al., 2015; Measures et al., 2008; Measures and Vink, 2000; Pohl et al., 2011; Schlosser et al., 2014), and also attributed to wet deposition . However, spatial variability in the distribution of dAl in the tropical Atlantic Ocean is a consequence of the sporadic and seasonal nature of mineral dust plumes with dust pulses varying in intensity on a daily basis (Patey et al., 2015) and with seasonal migration of the ITCZ.

25   ### 3.3.3 Dissolved Al in the surface mixed layer of the South East Atlantic Ocean (GA08)

Along GEOTRACES section GA08 in the South East Atlantic, dAl concentrations ranged from 1.2 (station 45) to 784 nM (station 15) (median 9 nM; n=44). The lowest dAl concentrations were found south of 20°S at stations along the prime meridian and at ca. 30°S and 1° to 10°E as a consequence of low aerosol deposition to the South Atlantic Gyre (SAG) region. Similar low concentrations of surface dAl associated with low productivity waters in the South Atlantic Gyre have

30   been reported (Measures, 1995). Low dAl concentrations (down to 1.3 nM) were observed during GA08 in the Benguela Coastal Current (BENG) region off Namibia coinciding with high Chl a concentrations (Figure S4) and thus enhanced dAl scavenging onto biogenic particles (Figure 3). The enhanced scavenging of dAl by particles is supported by elevated

concentrations of total dissolvable Al (unfiltered) during the AMT-6 cruise (Bowie et al., 2002). Bowie et al. (2002) argued that the enhanced total dissolvable Al was a consequence of Al-rich upwelled waters. Significant correlations between enhanced biogenic particles, and low dAl and high pAl concentrations have recently been reported (Menzel Barraqueta et al., 2018), indicating the control of biogenic particles on Al cycling in surface waters. The highest dAl concentrations (up to 784

5   nM) were observed along the SW African coast north of 6°S (stations 14 to 23) in the Guinean Current Coastal region (GUIN) and were associated with freshwater inputs from the Congo River. Similar observations were made by van Bennekom and Jager (1978), and enhanced levels of dAl (up to 50 nM) associated with inputs from the Congo river have been reportedd as far as 1200 km (6°S 0°E) from the river mouth (Van Der Loeff et al., 1997). Between the Congo River mouth (6°S) and the Angola-Benguela frontal zone (ca. 11°S) (Figure 1) elevated dAl was observed (20 – 40 nM) (Figure 3).

10 Possible sources for the elevated dAl concentrations are urban emissions and atmospheric mineral dust from West Africa. Prospero (1996a) argued that when the ITCZ migrates south of the equator, additional southward transfer to the Gulf of Guinea of atmospheric dust from the Sahara and the Sahel regions can occur during austral summer. In addition, the low Chl a concentrations in the GUIN region would facilitate dAl accumulation in the surface mixed layer due to a lack of adsorption onto biogenic particles.

15 **3.3.4 Dissolved Al in the surface mixed layer of the South Atlantic Ocean (GA10)**

Along GEOTRACES section GA10 in the South Atlantic Ocean, dAl concentrations were generally low and ranged between 0.3 nM in the SAC and 15.8 nM on the Argentine shelf ((n=17) median = 1.6 nM) (Figure 3). Highest concentrations (up to 16 nM) were observed on the South West Atlantic Shelf region (FKLD). The FKLD is thought to be influenced by dAl inputs from the River de la Plata, shelf sources, and possibly atmospheric deposition from Patagonian sources (Chance et al.,

20 2015; Jickells et al., 2005; Mahowald et al., 2005; Wagener et al., 2008). However, the correlation between surface salinity and dAl for the FKLD is weak (n=4, R^2=0.13) and suggests a minor influence on Al concentrations from freshwater sources. Thus, it is unlikely that the River de la Plata was a major source of dAl at the time of the cruise. An additional input of dAl could be associated from the advection Al rich waters of the southward flowing Brazil Current (Vink and Measures, 2001). However, this feature has been observed somewhat further north at 34°S and the influence of the Brazil Current at our

25 latitude may been counterbalanced by the northward flowing Malvinas Current (Figure 1). Similar dAl concentrations in the vicinity of the South American continent were observed during expedition ANT IX/1 (Van Der Loeff et al., 1997) and AMT-3 (Bowie et al., 2002) and attributed to recent dust deposition. In the South Subtropical Convergence region (SSTC), the dAl concentrations were low (<5 nM), reflecting low Al inputs from atmospheric deposition (Mahowald et al., 2005) and/or removal via particle scavenging in SSTC along ca. 40° S. Our observations agree with measurements of low concentration of

30 dAl in the high latitude South Atlantic (Middag et al., 2011).

3.3 Fractional solubility of Al ($Al_{sol\%}$):

The fractional solubility of trace metals from aerosols is controlled by: 1) chemical processing during atmospheric transport which is influenced by the balance of acid species (enhanced by anthropogenic sources e.g. fossil fuel combustion; (Ito, 2015; Sholkovitz et al., 2012) and the phase partitioning of NH_3 (Hennigan et al., 2015); and 2) composition and type of

5 particle; aerosols from different sources have different mineralogies and size distributions which influence the solubility of metals (Baker and Jickells, 2017). Reported aerosol Al fractional solubilities in aerosols span a large range from 0.5 to 100 % (Baker et al., 2006; Buck et al., 2010; Measures et al., 2010; Prospero et al., 1987; Shelley et al., 2017a). One of the reasons for this large range is likely the lack of standardisation in aerosol leaching methods (Aguilar-Islas et al., 2010). An up to twentyfold (1 to 20 g m^{-2} yr^{-1}) difference between atmospheric deposition fluxes estimated from Al fractional solubility

10 values following two different aerosol leaching methods has been reported by Anderson et al. (2016). However, based on aerosol Fe solubility experiments, the largest differences resulted from aerosols from different sources (Aguilar-Islas et al., 2010; Fishwick et al., 2014).

In an early study which used dAl concentrations in the surface mixed layer to derive atmospheric deposition fluxes, Measures and Brown (1996) choose an Al fractional solubility range of 1.5 to 5 % for the tropical Atlantic, with the upper

15 limit derived from aerosols and rain data by Prospero et al. (1987). Measures and Brown (1996) discussed that the chosen upper boundary for Al fractional solubility may have been too low, as earlier studies (Maring and Duce, 1987) reported an Al fractional solubility of 9 %, attributed to cloud processing during long-range atmospheric transport to the mid-Pacific Ocean, and thus not directly applicable to tropical Atlantic aerosols.

As our study region spans the entire Atlantic Ocean, we expect a large range in Al fractional solubility due to multiple

20 aerosol sources (Baker and Jickells, 2017; Baker et al., 2006). Table S3 shows the Al fractional solubility for each region and sub-region (Figure S2) and the relative abundance of air mass back trajectories. The Al fractional solubility partially reflects the different aerosol sources. The lowest Al fractional solubility values (5-7.7%) were calculated for the NTRA and WTRA in the tropical Atlantic (GA06) and for the GUIN and BENG region in the Southeast Atlantic (GA08) due to the dominance of mineral dust. The highest Al fractional solubility (11.6-21%) was calculated at high latitudes (GA01 and GA10) and in the

25 SATL (GA08) which was likely due to the greater distances from aerosol source regions and/or higher degree of atmospheric processing that these aerosols have undergone during transport (e.g. Shelley et al., 2018). Overall, the Al fractional solubility used in this study ranged from 5 to 21 %. The higher the Al fractional solubility value, the less aerosol material is required to maintain the observed dAl surface mixed layer concentrations.

3.4 Residence time of dAl

30 The residence time of dAl in the surface mixed layer is a balance between atmospheric, riverine and sedimentary inputs, and removal processes which are dominated by scavenging of dAl by biogenic particles (Orians and Bruland, 1986). Short residence times are associated with regions of enhanced mineral dust deposition (Dammshäuser et al., 2011; Schüßler et al.,

2005) such as the tropical North Atlantic and regions of enhanced biological activity (primary productivity) such as the North Atlantic (north of 40°N). In contrast, long Al residence times are associated with regions of low mineral dust deposition and low biological activity (Dammshäuser et al., 2011; Jickells, 1999) such as the South Atlantic subtropical gyre. The residence time of dAl in the upper ocean has been estimated to range from ~0.2 to more than 17 yr (Dammshäuser et al., 2011; Jickells, 1999; Jickells et al., 1994; Orians and Bruland, 1986) and up to 73 yr in modelling studies (Han et al., 2008). In this study, we used short Al residence times in the surface mixed layer for the North Atlantic (GA01), tropical Atlantic (GA06), along the upwelling regions in the Southeast Atlantic (GA08), and for the South Atlantic along the South Subtropical Convergence region (SSTC) (GA10). Longer Al residence times were used for the South East Atlantic Ocean, more precisely along the prime meridian as a consequence of low removal rates removal due to low primary productivity and low atmospheric deposition. Overall, the Al residence times used in this study (Table S5), and derived for each biogeochemical province from the estimates provided in Han et al. (2008), ranged between 0.75 and 3 years.

3.5 Application of the MADCOW model to derive total atmospheric deposition fluxes in the study area

3.5.1 MADCOW input parameter assumptions

The original MADCOW model (Measures and Brown, 1996) assumed a uniform residence time of 5 yr for dAl in the surface mixed layer, an invariant content of Al in dust of 8%, a fixed MLD of 30 m, and an aerosol Al fractional solubility between 1.5 and 5%. The total dust deposition was calculated by multiplying the concentration of dAl in the mixed layer by 0.133 and 0.04 (factors for unit conversion) for a solubility of 1.5 and 5 %, respectively. Our study region spans the whole Atlantic Ocean, with a range in MLDs, fractional Al solubilities, and residence times of Al in the surface mixed layer. The different input parameters used for the dust flux calculations for each of the four study regions can be found in Table S5 and relate to the factors described in Sections 2 and 3. Mixed layer depths were deeper for GA01 and GA10, and shallower for GA06 and GA08. The residence time of dAl in the surface mixed layer along the four transects was quite uniform and ranged from 0.75 to 3 years. The largest variability was noted for the aerosol Al fractional solubility due to inter-annual and inter-seasonal variability in the contribution of different aerosol sources, incomplete spatial coverage, wet to dry deposition balance, etc. As a consequence, for each cruise we have chosen a lower and upper limit of Al fractional solubility. As such we obtained an upper and lower range in atmospheric deposition fluxes for each cruise. The total range on aerosol Al fractional solubility used in this study was 5 to 20%, which is up to 3x and 4x higher than the lower and upper limit used by Measures and Brown (1996). Higher Al fractional solubilities were used for GA01 and GA10 and lower values for GA08 and GA06.

3.6 Atmospheric deposition fluxes

Figure 6 shows the average atmospheric deposition flux (wet + dry) for each station. In addition, Figure 5S (a, b, c and d) shows a comparison of calculated average total atmospheric aerosol deposition fluxes (this study) and total atmospheric deposition fluxes for each station extracted from the composite model of Mahowald et al. (2005). In Table 1, we present our

total atmospheric deposition fluxes values for each biogeochemical province compared to the model estimates from Mahowald et al. (2005) and (Duce et al., 1991). Overall we found good agreement along GA01, GA08, and GA10. Weaker agreement was found in the tropical Atlantic along GA06. In the following sections we describe our atmospheric deposition fluxes in more detail.

5 **3.6.1 Atmospheric deposition fluxes to the North Atlantic and Labrador Sea (GA01)**

In the North Atlantic, along the GA01 section, our calculated atmospheric deposition fluxes ranged from 1.75 ± 0.71 g m^{-2} yr^{-1} (St. 2) near the Iberian Peninsula in the NAST region to 0.12 ± 0.05 g m^{-2} yr^{-1} (St. 78) above the Newfoundland margin in the ARCT region. The average atmospheric deposition flux was 0.49 ± 0.46 g m^{-2} y^{-1} (Figure 6 and S5). The highest atmospheric deposition fluxes were calculated in the vicinity of land masses (i.e. Iberian Peninsula and Greenland) and could

10 be partly due to overestimations by the MADCOW model. An overestimation would arise if there were additional Al sources, rather than Al being input solely from atmospheric deposition. The coastal stations (1, 2 and 4; Figure S1) near the Iberian Peninsula received additional Al inputs from the Tagus estuary (Menzel Barraqueta et al., 2018), while the coastal stations (53 and 63; Figure S1) near Greenland are influenced by additional Al inputs from glacial run-off and ice melt (Menzel Barraqueta et al., 2018). With these stations removed, the average atmospheric deposition flux along GA01

15 decreased to 0.28 ± 0.12 g m^{-2} yr^{-1} (n=24). Although the atmospheric deposition fluxes near the Iberian Peninsula were high relative to the rest of the transect, they are comparable to modelled atmospheric aerosol deposition fluxes (Mahowald et al., 2005) (Table 1 and Figure S5a). Measures et al. (2015) reported an atmospheric deposition flux of ca. 0.91 g m^{-2} yr^{-1} (station USGT10-02) close to the Iberian Peninsula along GEOTRACES section GA03 (Figure 6), which is somewhat lower than our average deposition flux for stations 1, 2 and 4 (1.63 ± 0.08 g m^{-2} yr^{-1}). Our calculated fluxes derived from dAl at coastal

20 stations near the Iberian Peninsula may be on the high end of the scale due to additional Al inputs from the Tagus estuary which did not influence the nearby stations sampled by Measures et al. (2015). In the NAST we derived an average dust flux for stations 21, 23 and 25 of 0.42 ± 0.17 g m^{-2} yr^{-1} which is in good agreement with calculated atmospheric deposition fluxes for the same region during the 2003 CLIVAR A16N cruise (Measures et al., 2015) using aerosol Al concentrations from Buck et al. (2010) (Figure 6). Shelley et al. (2017b) reported atmospheric deposition fluxes for a suite of elements for the

25 GA01 cruise using two different approaches; 1) aerosol and precipitation concentration data (which they termed "traditional approach") and 2) [7]Be in aerosols and the surface mixed layer. They divided the GA01 section into two areas: (i) Area 1 = west of 30° W; (ii) Area 2 = east of 30° W (Figure 1). For Area 1 they derived atmospheric deposition fluxes of 0.03 and 0.1 g m^{-2} yr^{-1} using the traditional and [7]Be approaches, respectively. For Area 2, the atmospheric deposition fluxes were 0.19 and 0.14 g m^{-2} yr^{-1} for the traditional and [7]Be approaches, respectively. With the MADCOW model we calculated average

30 atmospheric deposition fluxes of 0.27 ± 0.16 and 0.3 ± 0.12 g m^{-2} yr^{-1} for Area 1 and 2, respectively. The average modelled flux estimates for the same areas from Mahowald et al., 2005 were 0.36 ± 0.03 and 0.76 ± 0.32 g m^{-2} yr^{-1}. It is encouraging that the different flux results are of a similar order of magnitude, although the dust flux estimates derived from Mahowald et al. (2005) were always highest. It is possible that the dust deposition model (Mahowald et al., 2005) may have overestimated

atmospheric deposition in the North Atlantic (north of 50°N) due to the limited number of field observations available at the time. Interestingly, a higher atmospheric aerosol deposition flux was calculated with the MADCOW model than with either the aerosol approach or the ^{7}Be method. This could be due to the different timescales over which each approach integrates. The MADCOW model approach integrates the total atmospheric deposition flux over a period of ca. 1 yr prior (based on our

5   choice of dAl surface mixed layer residence time) to the GA01 cruise, while the ^{7}Be approach integrates over a period of 3 months, and the aerosol approach provides a snapshot over a period of days. The elevated atmospheric deposition flux for the traditional compared to the ^{7}Be approach in area 2 was attributed to ^{7}Be scavenging onto biogenic particles near the Iberian Peninsula (Shelley et al., 2017).

3.6.2 Atmospheric deposition fluxes to the Tropical Atlantic (GA06)

10   Overall, the atmospheric deposition fluxes calculated for the tropical Atlantic using MADCOW are generally of the same order of magnitude compared to modelled atmospheric deposition fluxes (Mahowald et al., 2005) (Table 1 and Figure S5). Along GA06, the calculated atmospheric deposition fluxes ranged from 1.19 ± 0.45 g m^{-2} yr^{-1} at station 8 to 9.96 ± 3.72 g m^{-2} yr^{-1} at station 14 (Figure S1 and 6). The average calculated atmospheric deposition flux along the cruise was 3.46 ± 2.18 g m^{-2} yr^{-1}. Large discrepancies are observed between our MADCOW model results and the modelled atmospheric deposition

15   fluxes of Duce et al. (1991) (Figure 6) and Mahowald et al. (2005) (Figure S5). The largest differences are found in the NATR, along the East-West transect and north of 8°N (Figure S3b). Along the East-West transect (Station 7 to 9), at ca. 12°N, and north of 8°N, our atmospheric deposition fluxes ranged between 1.19 ± 0.44 and 3.54 ± 1.32 g m^{-2} yr^{-1} while modelled dust fluxes were above 8 g m^{-2} yr^{-1} and reach up to 12 g m^{-2} yr^{-1} (station 7). The discrepancy could result from differences in the solubility of aerosols in the east and west of the basin. A combination of more soluble aerosols transported

20   from mineral dust sources regions in North Africa via the trade winds to the western tropical Atlantic and from American sources may result in higher levels of dAl in the western tropical Atlantic than in the eastern tropical Atlantic (Measures et al., 2015; Sedwick et al., 2007). In addition, the Mahowald model uses extensive field data and monthly satellite retrievals over many years. Thus, the latter model may better capture the high degree of inter-annual and inter-seasonal variability in dust. Whilst there is more dust being deposited in the eastern tropical Atlantic than in the western tropical Atlantic,

25   MADCOW calculates higher atmospheric deposition fluxes in the western tropical Atlantic than in the eastern tropical Atlantic (this study and Measures et al., 2008; 2015). These results do not match the observations (from field data and satellite retrievals) and suggests that the MADCOW model is not able to accurately determine atmospheric deposition fluxes in the tropical North Atlantic Ocean. In contrast, in the WTRA, our average atmospheric deposition flux of 3.82 ± 2.72 g m^{-2} yr^{-1} agrees very well with modelled atmospheric deposition fluxes (4.4 ± 3.2 g m^{-2} yr^{-1}) (Duce et al., 1991; Mahowald et al.,

30   2005).

3.6.3 Atmospheric deposition fluxes to the South East Atlantic (GA08)

The MADCOW model most likely overestimates atmospheric aerosol deposition fluxes to the GUIN region north of 6°S with fluxes ranging between 38 to 163 g m^{-2} yr^{-1}. We have omitted stations 14 to 21 from the average atmospheric deposition flux, as they are strongly influenced by additional dAl inputs from the Congo River (Figure 1 and 3). Following this

5   removal, atmospheric deposition fluxes along GA08 (Figure 6) ranged from 0.04 ± 0.01 g m^{-2} yr^{-1} in the South Atlantic Gyre region (SATL) to 7.08 ± 1.44 g m^{-2} yr^{-1} in the Guinea Current Coastal region (GUIN) at ca. 12° S. The average calculated atmospheric deposition flux to the South East Atlantic was 1.33 ± 1.85 g m^{-2} yr^{-1}. The MADCOW model may underestimate atmospheric deposition fluxes in the BENG region, which is influenced by eastern boundary upwelling processes, supplying nutrients from deep to surface waters and resulting in enhance primary productivity with high levels of Chl a (Figure S4).

10 The BENG region receives mineral dust inputs from the Namib Desert (Prospero et al., 2002), but the large abundance of biogenic particles likely result in low surface dAl concentrations (< 7 nM) (Figure 3) due to enhance scavenging. Mahowald et al. (2005) calculated an average atmospheric deposition flux for the BENG region of 5.2 ± 4.16 g m^{-2} yr^{-1} with deposition values of up to 11.96 g m^{-2} yr^{-1} (station 48). However, our atmospheric deposition fluxes for this region are rather low with an average of 0.36 ± 0.18 g m^{-2} yr^{-1}. In contrast, our MADCOW derived atmospheric deposition fluxes in the SATL region

15 (0.17 ± 0.18 g m^{-2} yr^{-1}) are in close agreement with model estimates (0.22 ± 0.09 g m^{-2} yr^{-1}).

3.6.4 Atmospheric deposition fluxes to the South Atlantic Ocean (GA10)

Along GA10, the calculated atmospheric deposition fluxes ranged from 0.15 ± 0.1 g m^{-2} yr^{-1} in the South Subtropical Convergence (SSTC) region to 1.23 ± 0.67 g m^{-2} yr^{-1} in the South West Atlantic Shelf (FKLD) region off Argentina. The average atmospheric deposition flux calculated along the 40°S section was 0.41 ± 0.56 g m^{-2} yr^{-1}. The highest atmospheric

20 deposition flux was estimated in the FKLD, downwind from South America with Patagonian dust reported as the main source of mineral dust to the South Atlantic Ocean (Johnson et al., 2010; Wagener et al., 2008). Our atmospheric deposition fluxes in the FKLD agree with model estimates for the same region from Mahowald et al. (2005) (Table 1) and Wagener et al. (2008). Some discrepancies exist between the region of maximum atmospheric deposition. Indeed, Wagener et al. (2008) acknowledged this issue stating that the largest uncertainty in their estimates occurred downwind from South America as

25 their field data from this sector were collected on cruises in the South Pacific and South Indian Oceans. The lowest atmospheric aerosol deposition was found along the SSTC region (0.15 ± 0.1 g m^{-2} yr^{-1}) and were somewhat lower than model results (Mahowald et al., 2005) (0.44 ± 0.34 g m^{-2} yr^{-1}) but identical within the calculated uncertainties. In the EAFR, we calculated an average atmospheric deposition flux of 0.21 ± 0.22 g m^{-2} yr^{-1}. The latter flux agrees very well with total atmospheric deposition fluxes for the same region calculated from aerosol samples collected on the Falkland Islands (0.18 g

30 m^{-2} yr^{-1}) (Chance et al., 2015) and with model results (0.28 ± 0.14 g m^{-2} yr^{-1}) (Mahowald et al., 2005). It is possible that the South Atlantic Ocean also receives additional mineral dust inputs from South African sources although Patagonian dust is considered the major source of aerosols to this region (Gaiero et al., 2003; Wagener et al., 2008).

Biogeosciences
Discussions

EGU
Open Access

4 Conclusions

Dissolved Al concentrations in the surface ocean are a balance between input and removal processes. In this context, we can use the concentration of dAl in the mixed layer along with the residence time of dAl in the mixed layer to calculate atmospheric deposition fluxes. Overall, in oceanic regions beyond the shelf break, we found good agreement between our

5 calculated MADCOW atmospheric deposition fluxes and modelled atmospheric deposition fluxes (Mahowald et al., 2005). The agreement between our MADCOW deposition flux calculations and model results was poor in regions with additional Al inputs (e.g. river run off, ice melt, and benthic) and strong Al removal by biogenic particles in upwelling regions. Away from the main aerosol sources to the Atlantic Ocean, we found that our atmospheric deposition fluxes were lower than model fluxes which may suggest that these regions receive less atmospheric inputs than models indicate. As such, this work

10 provides new constrains for models of atmospheric deposition for the largely under-sampled regions of the Atlantic Ocean (e.g. Labrador Sea, South Atlantic and Southeast Atlantic Ocean). Specifically, (Mahowald et al., 2008) note that there are few aerosol measurements reported for the region between 30° and 60° S, due to a lack of island site for deployment of aerosol samplers and the remoteness of the region presenting logistical challenges for research cruises. In the GEOTRACES programme, a concerted effort has been made to cover these under-sampled regions of the ocean. Dissolved Al is a key trace

15 element of the GEOTRACES programme and as such it is measured on all the GEOTRACES cruises which implies a major strength of the approach used in this study. We acknowledge that there are regions of the Atlantic for which the application of the MADCOW model has limitations (i.e. tropical Atlantic Ocean). In these regions, more work is needed to constrain parameters such aerosol Al fractional solubility and the residence time of Al within the surface mixed layer. Realistic residence time values would significantly improve our atmospheric deposition flux results. We suggest that forthcoming

20 expeditions should use more than one technique to calculate atmospheric deposition fluxes as different methods provide us with complimentary information. The new Intermediate Data Product from the GEOTRACES Programme along with upcoming dAl datasets will give us a better coverage of under-sampled regions which combined with historical data will help us to refine atmospheric deposition fluxes (i.e. capturing seasonal and inter-annual variability).

Biogeosciences
Discussions

Open Access

EGU

5

References

Achterberg, E. P., Moore, C. M., Henson, S. A., Steigenberger, S., Stohl, A., Eckhardt, S., Avendano, L. C., Cassidy, M., Hembury, D.,
10 and Klar, J. K.: Natural iron fertilization by the Eyjafjallajökull volcanic eruption, Geophysical Research Letters, 40, 921-926, 2013.
Aguilar-Islas, A. M., Wu, J., Rember, R., Johansen, A. M., and Shank, L. M.: Dissolution of aerosol-derived iron in seawater: Leach solution chemistry, aerosol type, and colloidal iron fraction, Marine Chemistry, 120, 25-33, 2010.
Anderson, R. F., Cheng, H., Edwards, R. L., Fleisher, M. Q., Hayes, C. T., Huang, K.-F., Kadko, D., Lam, P. J., Landing, W. M., Lao, Y., Lu, Y., Measures, C. I., Moran, S. B., Morton, P. L., Ohnemus, D. C., Robinson, L. F., and Shelley, R. U.: How well can we quantify dust
15 deposition to the ocean?, Philosophical Transactions of the Royal Society A: Mathematical,   Physical and Engineering Sciences, 374, 2016.
Baker, A., Adams, C., Bell, T., Jickells, T., and Ganzeveld, L.: Estimation of atmospheric nutrient inputs to the Atlantic Ocean from 50° N to 50° S based on large-scale field sampling: Iron and other dust-associated elements, Global Biogeochemical Cycles, 27, 755-767, 2013.
Baker, A. R. and Croot, P. L.: Atmospheric and marine controls on aerosol iron solubility in seawater, Marine Chemistry, 120, 4-13, 2010.
20 Baker, A. R. and Jickells, T. D.: Atmospheric deposition of soluble trace elements along the Atlantic Meridional Transect (AMT), Progress in Oceanography, 158, 41-51, 2017.
Baker, A. R., Jickells, T. D., Witt, M., and Linge, K. L.: Trends in the solubility of iron, aluminium, manganese and phosphorus in aerosol collected over the Atlantic Ocean, Marine Chemistry, 98, 43-58, 2006.
Baker, A. R., Kelly, S. D., Biswas, K. F., Witt, M., and Jickells, T. D.: Atmospheric deposition of nutrients to the Atlantic Ocean,
25 Geophysical Research Letters, 30, 2296, 2003.
Barrett, P. M., Resing, J. A., Buck, N. J., Landing, W. M., Morton, P. L., and Shelley, R. U.: Changes in the distribution of Al and particulate Fe along A16N in the eastern North Atlantic Ocean between 2003 and 2013: Implications for changes in dust deposition, Marine Chemistry, 177, 57-68, 2015.
Bowie, A. R., Whitworth, D. J., Achterberg, E. P., Mantoura, R. F. C., and Worsfold, P. J.: Biogeochemistry of Fe and other trace elements
30 (Al, Co, Ni) in the upper Atlantic Ocean, Deep Sea Research Part I: Oceanographic Research Papers, 49, 605-636, 2002.
Brown, M. T. and Bruland, K. W.: An improved flow-injection analysis method for the determination of dissolved aluminum in seawater, Limnol. Oceanogr. Methods, 6, 87-95, 2008.
Buck, C. S., Landing, W. M., Resing, J. A., and Measures, C. I.: The solubility and deposition of aerosol Fe and other trace elements in the north atlantic ocean: observations from the A16N CLIVAR/CO 2 repeat hydrography section, Marine Chemistry, 120, 57-70, 2010.
35 Bullard, J. E., Baddock, M., Bradwell, T., Crusius, J., Darlington, E., Gaiero, D., Gasso, S., Gisladottir, G., Hodgkins, R., and McCulloch, R.: High-latitude dust in the Earth system, Reviews of Geophysics, 54, 447-485, 2016.
Chahine, M. T.: The hydrological cycle and its influence on climate, Nature, 359, 373, 1992.
Chance, R., Jickells, T. D., and Baker, A. R.: Atmospheric trace metal concentrations, solubility and deposition fluxes in remote marine air over the south-east Atlantic, Marine Chemistry, 177, 45-56, 2015.
40 Dammshäuser, A., Wagener, T., and Croot, P. L.: Surface water dissolved aluminum and titanium: Tracers for specific time scales of dust deposition to the Atlantic?, Geophysical Research Letters, 38, 2011.
Duce, R., Liss, P., Merrill, J., Atlas, E., Buat-Menard, P., Hicks, B., Miller, J., Prospero, J., Arimoto, R., and Church, T.: The atmospheric input of trace species to the world ocean, Global biogeochemical cycles, 5, 193-259, 1991.
Duce, R. A. and Tindale, N. W.: Atmospheric Transport of Iron and Its Deposition in the Ocean, Limnology and Oceanography, 36, 1715-
45 1726, 1991.
Fishwick, M. P., Sedwick, P. N., Lohan, M. C., Worsfold, P. J., Buck, K. N., Church, T. M., and Ussher, S. J.: The impact of changing surface ocean conditions on the dissolution of aerosol iron, Global Biogeochemical Cycles, 28, 1235-1250, 2014.

Gaiero, D. M., Probst, J. L., Depetris, P. J., Bidart, S. M., and Leleyter, L.: Iron and other transition metals in Patagonian riverborne and windborne materials: geochemical control and transport to the southern South Atlantic Ocean, Geochimica et Cosmochimica Acta, 67, 3603-3623, 2003.

Han, Q., Moore, J. K., Zender, C., Measures, C., and Hydes, D.: Constraining oceanic dust deposition using surface ocean dissolved Al, Global biogeochemical cycles, 22, 2008.

Hennigan, C., Izumi, J., Sullivan, A., Weber, R., and Nenes, A.: A critical evaluation of proxy methods used to estimate the acidity of atmospheric particles, Atmospheric Chemistry and Physics, 15, 2775, 2015.

Holte, J., Talley, L. D., Gilson, J., and Roemmich, D.: An Argo mixed layer climatology and database, Geophysical Research Letters, 2017. 2017.

Huneeus, N., Schulz, M., Balkanski, Y., Griesfeller, J., Prospero, M., Kinne, S., Bauer, S., Boucher, O., Chin, M., and Dentener, F.: Global dust model intercomparison in AeroCom phase I, Atmospheric Chemistry and Physics, 11, 7781-7816, 2011.

Hydes, D. and Liss, P.: Fluorimetric method for the determination of low concentrations of dissolved aluminium in natural waters, Analyst, 101, 922-931, 1976.

Ito, A.: Atmospheric processing of combustion aerosols as a source of bioavailable iron, Environmental Science & Technology Letters, 2, 70-75, 2015.

Jickells, T.: The inputs of dust derived elements to the Sargasso Sea; a synthesis, Marine Chemistry, 68, 5-14, 1999.

Jickells, T., Boyd, P., and Hunter, K. A.: Biogeochemical impacts of dust on the global carbon cycle. In: Mineral Dust, Springer, 2014.

Jickells, T., Church, T., Veron, A., and Arimoto, R.: Atmospheric inputs of manganese and aluminium to the Sargasso Sea and their relation to surface water concentrations, Marine chemistry, 46, 283-292, 1994.

Jickells, T., Dorling, S., Deuser, W., Church, T., Arimoto, R., and Prospero, J.: Air-borne dust fluxes to a deep water sediment trap in the Sargasso Sea, Global Biogeochemical Cycles, 12, 311-320, 1998.

Jickells, T. D., An, Z. S., Andersen, K. K., Baker, A. R., Bergametti, G., Brooks, N., Cao, J. J., Boyd, P. W., Duce, R. A., Hunter, K. A., Kawahata, H., Kubilay, N., laRoche, J., Liss, P. S., Mahowald, N., Prospero, J. M., Ridgwell, A. J., Tegen, I., and Torres, R.: Global iron connections between desert dust, ocean biogeochemistry, and climate, Science, 308, 67-71, 2005.

Johnson, M. S., Meskhidze, N., Solmon, F., Gassó, S., Chuang, P. Y., Gaiero, D. M., Yantosca, R. M., Wu, S., Wang, Y., and Carouge, C.: Modeling dust and soluble iron deposition to the South Atlantic Ocean, Journal of Geophysical Research: Atmospheres, 115, 2010.

Kadko, D., Landing, W. M., and Shelley, R. U.: A novel tracer technique to quantify the atmospheric flux of trace elements to remote ocean regions, Journal of Geophysical Research: Oceans, 120, 848-858, 2015.

Kadko, D. and Prospero, J.: Deposition of 7Be to Bermuda and the regional ocean: environmental factors affecting estimates of atmospheric flux to the ocean, Journal of Geophysical Research: Oceans, 116, 2011.

Kara, A. B., Rochford, P. A., and Hurlburt, H. E.: Mixed layer depth variability over the global ocean, Journal of Geophysical Research: Oceans, 108, 2003.

Kim, G. and Church, T. M.: Wet deposition of trace elements and radon daughter systematics in the South and equatorial Atlantic atmosphere, Global biogeochemical cycles, 16, 2002.

Kohfeld, K. E. and Harrison, S. P.: DIRTMAP: the geological record of dust, Earth-Science Reviews, 54, 81-114, 2001.

Longhurst, A. R.: Ecological geography of the sea, Academic Press, 2010.

Mahowald, N., Albani, S., Kok, J. F., Engelstaeder, S., Scanza, R., Ward, D. S., and Flanner, M. G.: The size distribution of desert dust aerosols and its impact on the Earth system, Aeolian Research, 15, 53-71, 2014.

Mahowald, N., Ward, D. S., Kloster, S., Flanner, M. G., Heald, C. L., Heavens, N. G., Hess, P. G., Lamarque, J.-F., and Chuang, P. Y.: Aerosol impacts on climate and biogeochemistry, Annual review of environment and resources, 36, 2011.

Mahowald, N. M., Baker, A. R., Bergametti, G., Brooks, N., Duce, R. A., Jickells, T. D., Kubilay, N., Prospero, J. M., and Tegen, I.: Atmospheric global dust cycle and iron inputs to the ocean, Global Biogeochemical Cycles, 19, 2005.

Mahowald, N. M., Engelstaedter, S., Luo, C., Sealy, A., Artaxo, P., Benitez-Nelson, C., Bonnet, S., Chen, Y., Chuang, P. Y., and Cohen, D. D.: Atmospheric iron deposition: global distribution, variability, and human perturbations, 2008. 2008.

Maring, H., Savoie, D., Izaguirre, M., Custals, L., and Reid, J.: Mineral dust aerosol size distribution change during atmospheric transport, Journal of Geophysical Research: Atmospheres, 108, 2003.

Maring, H. B. and Duce, R. A.: The impact of atmospheric aerosols on trace metal chemistry in open ocean surface seawater, 1. Aluminum, Earth and Planetary Science Letters, 84, 381-392, 1987.

Martin, J. H., Gordon, M., and Fitzwater, S. E.: The case for iron, Limnology and Oceanography, 36, 1793-1802, 1991.

Measures, C.: The distribution of Al in the IOC stations of the eastern Atlantic between 30° S and 34° N, Marine chemistry, 49, 267-281, 1995.

Measures, C., Hatta, M., Fitzsimmons, J., and Morton, P.: Dissolved Al in the zonal N Atlantic section of the US GEOTRACES 2010/2011 cruises and the importance of hydrothermal inputs, Deep Sea Research Part II: Topical Studies in Oceanography, 116, 176-186, 2015.

Measures, C., Landing, W., Brown, M., and Buck, C.: High-resolution Al and Fe data from the Atlantic Ocean CLIVAR-CO2 Repeat Hydrography A16N transect: Extensive linkages between atmospheric dust and upper ocean geochemistry, Global Biogeochemical Cycles, 22, 2008.

Measures, C., Sato, T., Vink, S., Howell, S., and Li, Y.: The fractional solubility of aluminium from mineral aerosols collected in Hawaii
5 and implications for atmospheric deposition of biogeochemically important trace elements, Marine Chemistry, 120, 144-153, 2010.

Measures, C. and Vink, S.: On the use of dissolved aluminum in surface waters to estimate dust deposition to the ocean, Global biogeochemical cycles, 14, 317-327, 2000.

Measures, C. I. and Brown, E. T.: Estimating Dust Input to the Atlantic Ocean Using Surface Water Aluminium Concentrations. In: The Impact of Desert Dust Across the Mediterranean, Guerzoni, S. and Chester, R. (Eds.), Springer Netherlands, Dordrecht, 1996.

10 Menzel Barraqueta, J. L., Schlosser, C., Planquette, H., Gourain, A., Cheize, M., Boutorh, J., Shelley, R., Pereira Contreira, L., Gledhill, M., Hopwood, M. J., Lherminier, P., Sarthou, G., and Achterberg, E. P.: Aluminium in the North Atlantic Ocean and the Labrador Sea (GEOTRACES GA01 section): roles of continental inputs and biogenic particle removal, Biogeosciences Discuss., 2018, 1-28, 2018.

Middag, R., Van Hulten, M., Van Aken, H., Rijkenberg, M., Gerringa, L., Laan, P., and De Baar, H.: Dissolved aluminium in the ocean conveyor of the West Atlantic Ocean: effects of the biological cycle, scavenging, sediment resuspension and hydrography, Marine
15 Chemistry, 177, 69-86, 2015.

Middag, R., van Slooten, C., de Baar, H. J. W., and Laan, P.: Dissolved aluminium in the Southern Ocean, Deep Sea Research Part II: Topical Studies in Oceanography, 58, 2647-2660, 2011.

Monterey, G. I. and Levitus, S.: Seasonal variability of mixed layer depth for the world ocean, US Department of Commerce, National Oceanic and Atmospheric Administration, National Environmental Satellite, Data, and Information Service, 1997.

20 Moore, C. M., Mills, M. M., Achterberg, E. P., Geider, R. J., LaRoche, J., Lucas, M. I., McDonagh, E. L., Pan, X., Poulton, A. J., and Rijkenberg, M. J.: Large-scale distribution of Atlantic nitrogen fixation controlled by iron availability, Nature Geoscience, 2, 867-871, 2009.

Moore, J. K., Doney, S. C., and Lindsay, K.: Upper ocean ecosystem dynamics and iron cycling in a global three-dimensional model, Global Biogeochemical Cycles, 18, 2004.

25 Orians, K. J. and Bruland, K. W.: The biogeochemistry of aluminum in the Pacific Ocean, Earth and planetary science letters, 78, 397-410, 1986.

Ott, S., Ott, A., Martin, D., and Young, J.: Analysis of a trans-Atlantic Saharan dust outbreak based on satellite and GATE data, Monthly Weather Review, 119, 1832-1850, 1991.

Patey, M. D., Achterberg, E. P., Rijkenberg, M. J., and Pearce, R.: Aerosol time-series measurements over the tropical Northeast Atlantic
30 Ocean: Dust sources, elemental composition and mineralogy, Marine Chemistry, 174, 103-119, 2015.

Pohl, C., Croot, P. L., Hennings, U., Daberkow, T., Budeus, G., and Loeff, M. R. v. d.: Synoptic transects on the distribution of trace elements (Hg, Pb, Cd, Cu, Ni, Zn, Co, Mn, Fe, and Al) in surface waters of the Northern- and Southern East Atlantic, Journal of Marine Systems, 84, 28-41, 2011.

Prospero, J.: Saharan dust transport over the North Atlantic Ocean and Mediterranean: an overview. In: The impact of desert dust across
35 the Mediterranean, Springer, 1996a.

Prospero, J. M.: The atmospheric transport of particles to the ocean, Scope-scientific committee on problems of the environment international council of Scientific unions, 57, 19-52, 1996b.

Prospero, J. M. and Carlson, T. N.: Vertical and areal distribution of Saharan dust over the western equatorial North Atlantic Ocean, Journal of Geophysical Research, 77, 5255-5265, 1972.

40 Prospero, J. M., Ginoux, P., Torres, O., Nicholson, S. E., and Gill, T. E.: Environmental characterization of global sources of atmospheric soil dust derived from the nimbus7 toms absorbing aerosol product, rev, 2002.

Prospero, J. M., Landing, W. M., and Schulz, M.: African dust deposition to Florida: Temporal and spatial variability and comparisons to models, Journal of Geophysical Research: Atmospheres, 115, n/a-n/a, 2010.

Prospero, J. M., Nees, R. T., and Uematsu, M.: Deposition rate of particulate and dissolved aluminum derived from Saharan dust in
45 precipitation at Miami, Florida, Journal of Geophysical Research: Atmospheres, 92, 14723-14731, 1987.

Resing, J. A. and Measures, C. I.: Fluorometric Determination of Al in Seawater by Flow Injection Analysis with In-Line Preconcentration, Analytical Chemistry, 66, 4105-4111, 1994.

Risien, C. M. and Chelton, D. B.: A global climatology of surface wind and wind stress fields from eight years of QuikSCAT scatterometer data, Journal of Physical Oceanography, 38, 2379-2413, 2008.

50 Sarthou, G., Baker, A. R., Blain, S., Achterberg, E. P., Boye, M., Bowie, A. R., Croot, P., Laan, P., de Baar, H. J. W., Jickells, T. D., and Worsfold, P. J.: Atmospheric iron deposition and sea-surface dissolved iron concentrations in the eastern Atlantic Ocean, Deep Sea Research Part I: Oceanographic Research Papers, 50, 1339-1352, 2003.

Schanze, J. J., Schmitt, R. W., and Yu, L.: The global oceanic freshwater cycle: A state-of-the-art quantification, Journal of Marine Research, 68, 569-595, 2010.

Schlosser, C., Klar, J. K., Wake, B. D., Snow, J. T., Honey, D. J., Woodward, E. M. S., Lohan, M. C., Achterberg, E. P., and Moore, C. M.: Seasonal ITCZ migration dynamically controls the location of the (sub)tropical Atlantic biogeochemical divide, Proceedings of the National Academy of Sciences, 111, 1438-1442, 2014.

Schüßler, U., Balzer, W., and Deeken, A.: Dissolved Al distribution, particulate Al fluxes and coupling to atmospheric Al and dust
5   deposition in the Arabian Sea, Deep Sea Research Part II: Topical Studies in Oceanography, 52, 1862-1878, 2005.

Sedwick, P. N., Sholkovitz, E. R., and Church, T. M.: Impact of anthropogenic combustion emissions on the fractional solubility of aerosol iron: Evidence from the Sargasso Sea, Geochemistry, Geophysics, Geosystems, 8, 2007.

Shelley, R. U., Landing, W. M., Ussher, S. J., Planquette, H., and Sarthou, G.: Characterisation of aerosol provenance from the fractional solubility of Fe (Al, Ti, Mn, Co, Ni, Cu, Zn, Cd and Pb) in North Atlantic aerosols (GEOTRACES cruises GA01 and GA03) using a two
10   stage leach, Biogeosciences Discuss., 2017, 1-31, 2017a.

Shelley, R. U., Roca-Martí, M., Castrillejo, M., Masqué, P., Landing, W. M., Planquette, H., and Sarthou, G.: Quantification of trace element atmospheric deposition fluxes to the Atlantic Ocean (> 40° N; GEOVIDE, GEOTRACES GA01) during spring 2014, Deep Sea Research Part I: Oceanographic Research Papers, 119, 34-49, 2017b.

Sholkovitz, E. R., Sedwick, P. N., Church, T. M., Baker, A. R., and Powell, C. F.: Fractional solubility of aerosol iron: Synthesis of a
15   global-scale data set, Geochimica et cosmochimica acta, 89, 173-189, 2012.

Slinn, S. and Slinn, W.: Predictions for particle deposition on natural waters, Atmospheric Environment (1967), 14, 1013-1016, 1980.

van Bennekom, A. J. and Jager, J. E.: Dissolved aluminium in the Zaire river plume, Netherlands Journal of Sea Research, 12, 358-367, 1978.

Van Der Loeff, M. R., Helmers, E., and Kattner, G.: Continuous transects of cadmium, copper, and aluminium in surface waters of the
20   Atlantic Ocean, 50°N to 50°S: correspondence and contrast with nutrient-like behaviour, Geochimica et Cosmochimica Acta, 61, 47-61, 1997.

van Hulten, M. M. P., Sterl, A., Tagliabue, A., Dutay, J. C., Gehlen, M., de Baar, H. J. W., and Middag, R.: Aluminium in an ocean general circulation model compared with the West Atlantic Geotraces cruises, Journal of Marine Systems, 126, 3-23, 2013.

Vink, S. and Measures, C. I.: The role of dust deposition in determining surface water distributions of Al and Fe in the South West
25   Atlantic, Deep Sea Research Part II: Topical Studies in Oceanography, 48, 2787-2809, 2001.

Wagener, T., Guieu, C., Losno, R., Bonnet, S., and Mahowald, N.: Revisiting atmospheric dust export to the Southern Hemisphere ocean: Biogeochemical implications, Global Biogeochemical Cycles, 22, 2008.

Webster, P. J.: The role of hydrological processes in ocean-atmosphere interactions, Reviews of Geophysics, 32, 427-476, 1994.

Yoo, J.-M. and Carton, J. A.: Annual and interannual variation of the freshwater budget in the tropical Atlantic Ocean and the Caribbean
30   Sea, Journal of physical Oceanography, 20, 831-845, 1990.

Yu, L. and Weller, R. A.: Objectively analyzed air–sea heat fluxes for the global ice-free oceans (1981–2005), Bulletin of the American Meteorological Society, 88, 527-539, 2007.

Zender, C. S., Bian, H., and Newman, D.: Mineral Dust Entrainment and Deposition (DEAD) model: Description and 1990s dust climatology, Journal of Geophysical Research: Atmospheres (1984–2012), 108, 2003.

35   Zhang, Y., Mahowald, N., Scanza, R., Journet, E., Desboeufs, K., Albani, S., Kok, J., Zhuang, G., Chen, Y., and Cohen, D.: Modeling the global emission, transport and deposition of trace elements associated with mineral dust, Biogeosciences (BG), 12, 5771-5792, 2015.
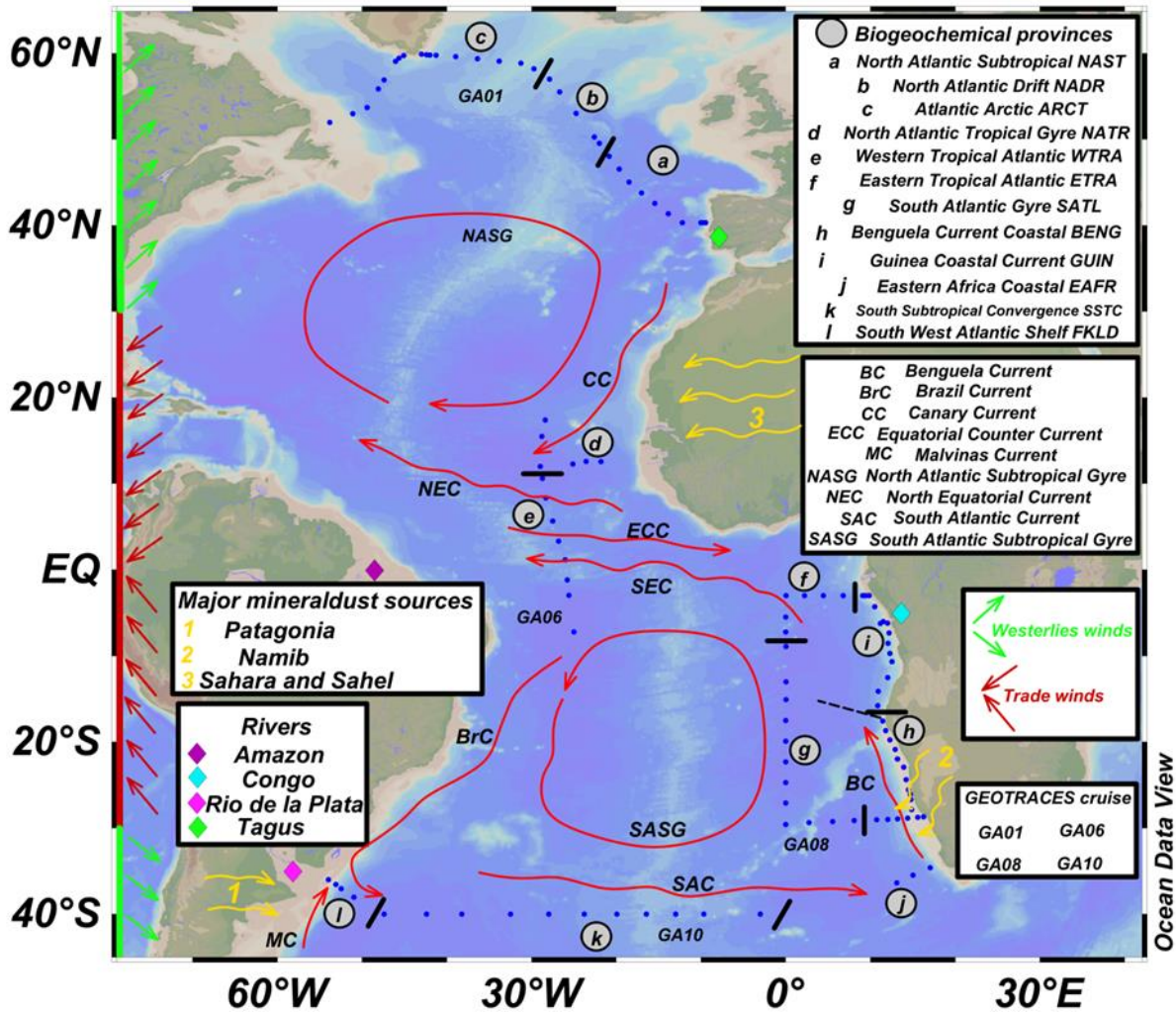
Figure 1: Map showing the location of the four GEOTRACES cruises. Red lines represent the main surface ocean currents. The diamond´s represent rivers. Yellow arrows represent approximate areas which act as the main mineral dust sources to the Atlantic ocean (Prospero et al., 2002). The yellow solid lines represent the area were maximum rainfall is associated with the ITCZ. Black lines divide different biogeochemical provinces used in this study which are labelled with letters. For station numbers for each cruise please refer to Figure S1.
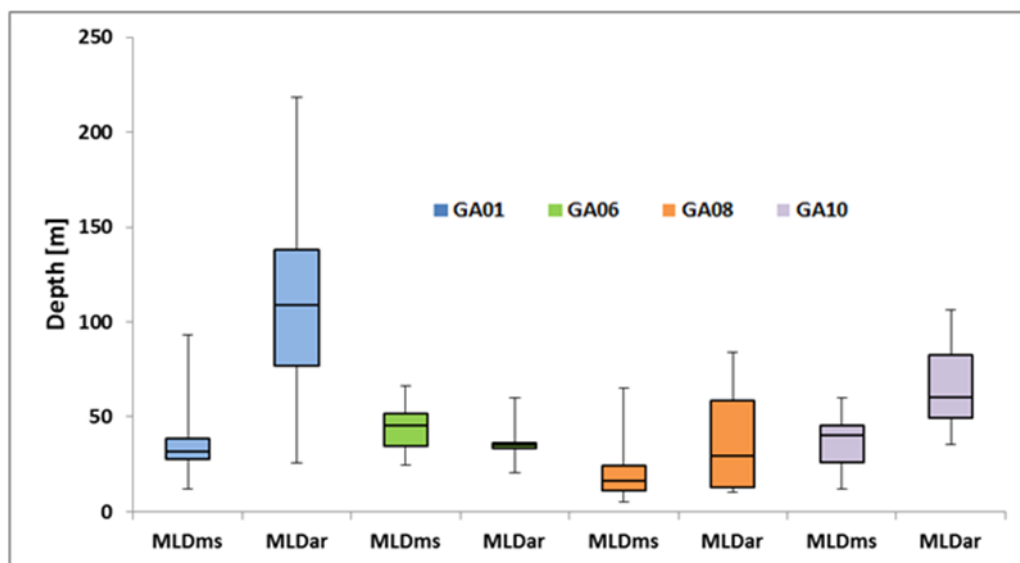
Figure 2: Box whisker plot for the MLD determined using in situ measurements (MLDms) and mixed layer climatology (MLDar) (http://mixedlayer.ucsd.edu/) (Holte et al., 2017).
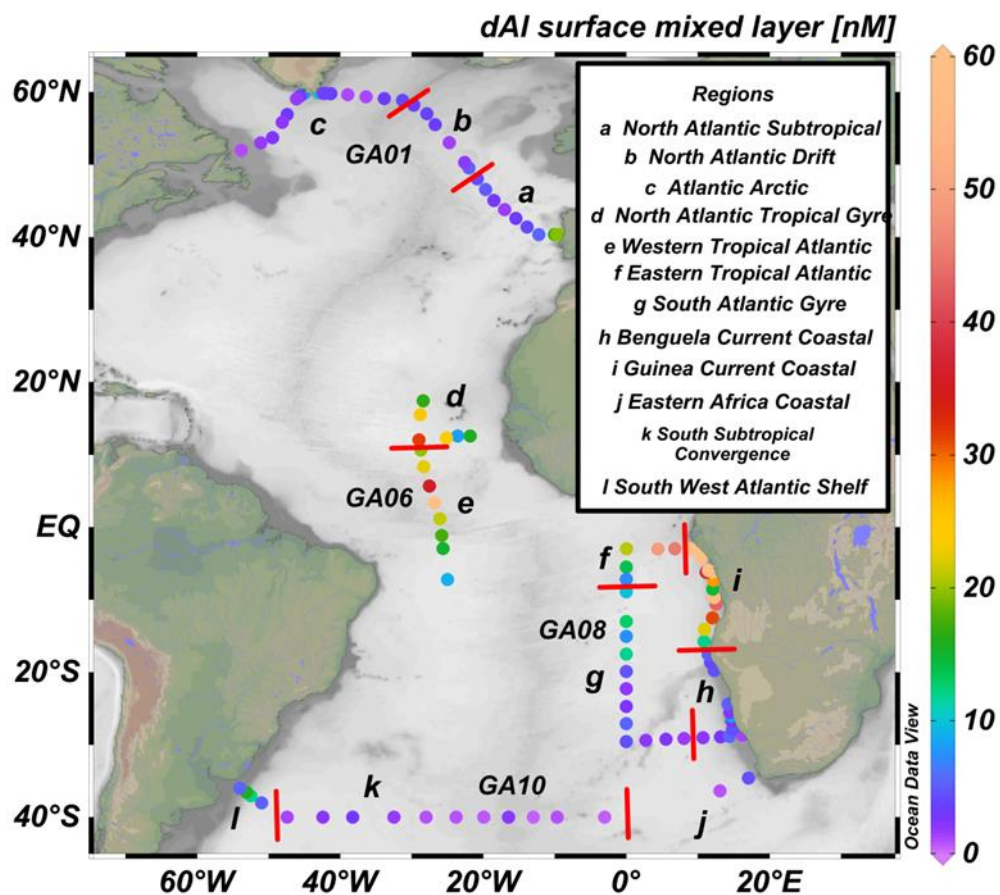
Figure 3: Surface mixed layer dAl concentrations (nM) for the cruises used in this study. Red lines divide the different biogeochemical provinces used in this study.
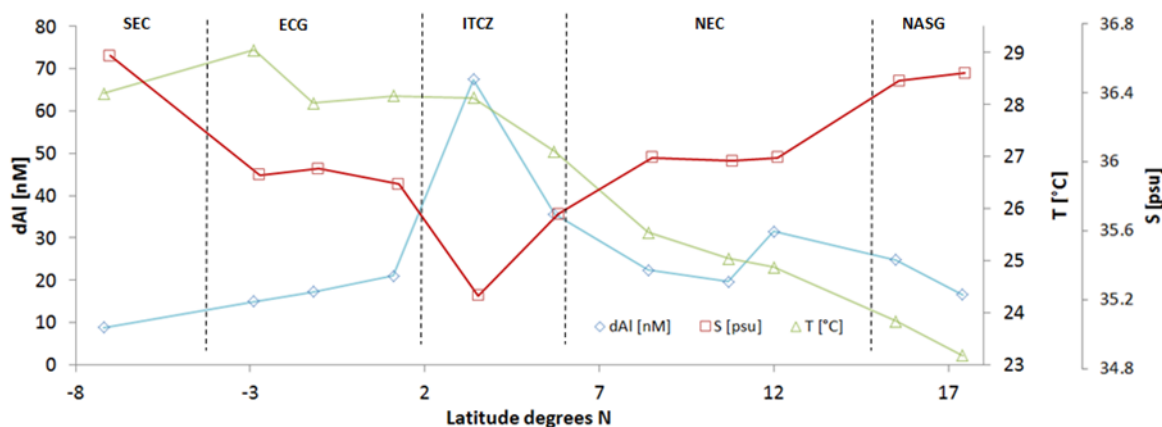
5

Figure 4 Distribution of dAl (nM), salinity and temperature for the northward transect in the tropical Atlantic (GA06). SEC, South Equatorial Current; ECG, Equatorial Gyre; ITCY, Intertropical Convergence Zone; NEC, North Equatorial Current; NASG, North Atlantic Subtropical Gyre.
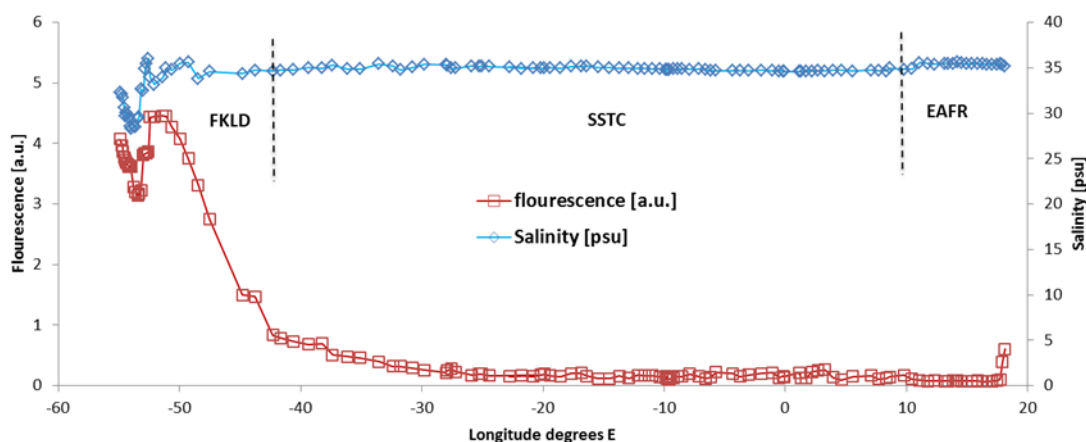
5

Figure 5: Salinity and fluorescence measurements from the ship sensors along the South Atlantic (GA10). FKLD, South West Atlantic Shelf region; SSTC, South Subtropical Convergence region; EAFR, Eastern Africa Coastal region.
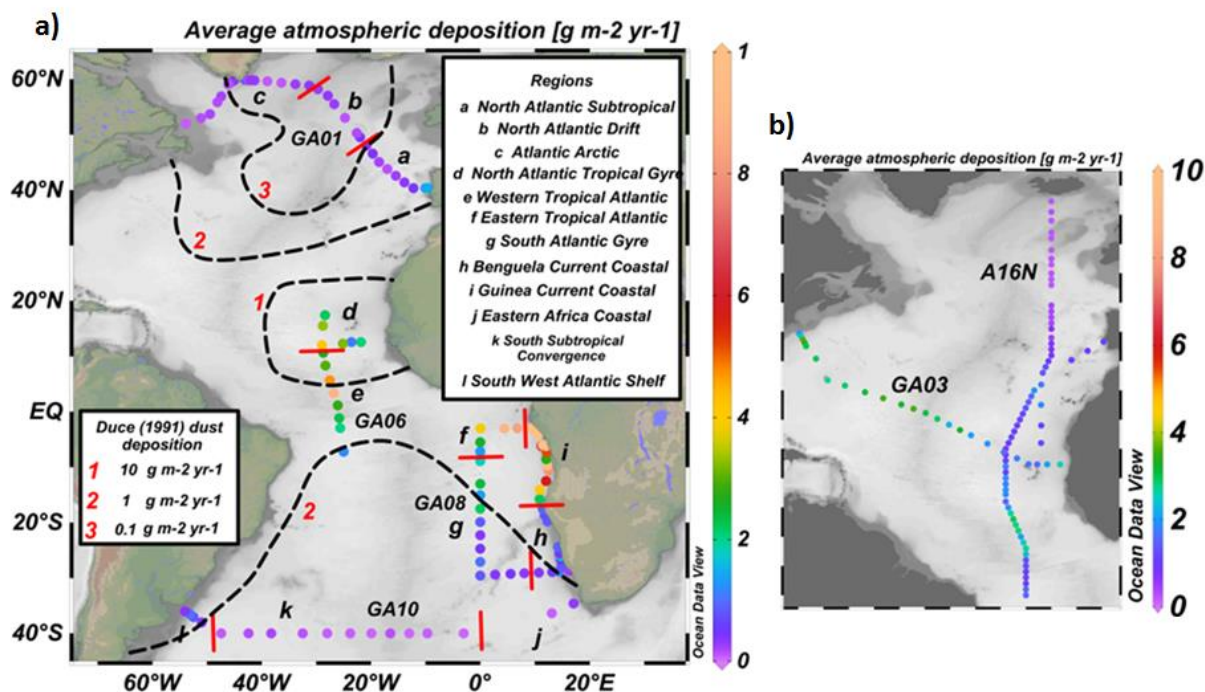
10

15

Figure 6: a) Average atmospheric deposition fluxes determined for the four GEOTRACES cruises. b) Average atmospheric deposition fluxes determined from GEOTRACES GA03 and A16N-2003 cruises are plotted (Measures et al., 2015). Black dashed lines defined boundaries of atmospheric aerosol deposition from (Duce et al., 1991).

5

Table 1: Average aerosol deposition fluxes estimated for each biogeochemical province. For reference on the different regions please refer to table S1. The deposition fluxes are given in g m^{-2} yr^{-1}. Mahowald and Duce refer to the atmospheric aerosol flux results provided in Mahowald et al., (2005) and Duce et al., (1991), respectively. GUIN* refers to deposition results affected with addition Al inputs from the Congo River plume.

10

15

Cruise	Biogeochemical province	Deposition (this study)	Mahowald	Duce
GA01	NAST	0.71 ± 0.65	1.05 ± 0.24	0.1 - 1
GA01	NADR	0.28 ± 0.12	0.52 ± 0.1	0.01 - 0.1
GA01	ARCT	0.27 ± 0.13	0.35 ± 0.03	0.01 - 1
GA06	NATR	2.2 ± 1.2	10 ± 1.3	10 - 100
GA06	WTRA	3.8 ± 2.7	4.4 ± 3.2	1 - 100
GA08	ETRA	2.65 ± 1.84	0.89 ± 0.36	1 - 10
GA08	GUIN* GUIN	26.2 ± 43.42 2.67 ± 1.96	1.04 ± 0.9	1 - 10
GA08	BENG	0.36 ± 0.18	5.2 ± 4.16	1 - 10
GA08	SATL	0.17 ± 0.18	0.22 ± 0.09	0.1 - 1
GA10	EAFR	0.21 ± 0.22	0.28 ± 0.14	0.1 - 1
GA10	SSTZ	0.15 ± 0.1	0.44 ± 0.34	0.1 - 1
GA10	FKLD	1.23 ± 0.67	1.17 ± 0.16	1 - 10